Release of K, Cl, and S during Pyrolysis and Combustion of High-Chlorine Biomass

Johansen, Joakim Myung; Jakobsen, Jon Geest; Frandsen, Flemming; Glarborg, Peter

Published in:
Energy & Fuels

Link to article, DOI:
10.1021/ef201098n

Publication date:
2011

Document Version
Publisher's PDF, also known as Version of record

energy&fuels

ARTICLE

pubs.acs.org/EF

Release of K, Cl, and S during Pyrolysis and Combustion of High-Chlorine Biomass

Joakim M. Johansen, Jon G. Jakobsen, Flemming J. Frandsen, and Peter Glarborg*

Department of Chemical and Biochemical Engineering, Technical University of Denmark, 2800 Kongens Lyngby, Denmark

ABSTRACT: The release of critical ash-forming elements during the pyrolysis and combustion of corn stover has been investigated through controlled lab-scale experiments supported by multicomponent and multiphase thermodynamic equilibrium calculations. Fuel samples were treated under isothermal conditions ranging from 500 to 1150 °C, under both pyrolysis and combustion atmospheres. The volatilized material was quantified by means of mass balances based on char and ash elemental analysis, compared to a corresponding feedstock fuel analysis. Close relations between the observed K and Cl release are found, suggesting that Cl is the main facilitator for K release through sublimation of KCl, determined to begin as the reaction temperature approaches 700−800 °C. K is present in abundance relative to Cl, and the K release is found to cease as the fuel reaches complete dechlorination. In addition, around 50 wt % of the Cl is released at temperatures below 500 °C, presumably as HCl formed through ion-exchange reactions with functional groups in the organic matrix. Complete dechlorination was achieved under combustion conditions as the temperature exceeded 800 °C. Approximately 50 wt % of the feedstock S is released at temperatures below 500 °C. This low-temperature release is related to the decomposition of the organic matrix, releasing the organically associated S. Under combustion conditions, the S release increases gradually at temperatures exceeding 800 °C, eventually reaching complete desulfurization at 1150 °C. The silicate/alumina chemistry is found to play a significant role in the alkali retention. The Si-rich sample is capable of retaining all excess K not released as KCl.

INTRODUCTION

Relying on the same basic principles as solid fossil fuel combustion, the thermal conversion of biomass fuels can draw on the knowledge gained from centuries of heat and power production using this technology. However, replacing conventional fossil fuels with biomass introduces a range of obstacles that need to be overcome. The primary issue is related to severe deposit formation and subsequent active corrosion when firing with biomass fuel especially rich in K, Cl, and S.[1−13]

Table 1 compares the elemental analysis of various solid fuels. Corn stover stands out with a high content of both Cl and K, especially compared to wood chips and coal. In addition, the corn stover contains moderate amounts of S, which all together makes the implementation of corn stover in full scale facilities difficult because of the potential corrosive, fouling, and aerosol forming effects due to inorganic release.

This work will primarily focus on the release characteristics of K, Cl, and S during the pyrolysis and combustion of Spanish corn stover. An estimated 28 million tons of corn stover with an approximate higher heating value of 18 MJ/kg are produced annually in Europe, making it abundant and relevant for energy exploitation. However, the high alkali and Cl contents have, so far, limited its use in medium to large scale power plants, and it is important to improve our knowledge of the transformation of critical ash forming elements.

Potassium Release Path. The release of K is complex, being closely related to the presence and transformation of especially Cl, Si, and S. Figure 1 summarizes the reaction paths and possible release mechanisms of K identified from a literature review conducted by the authors. The scheme is based on the work of van Lith,[3] who investigated the release of inorganic matter during the combustion of woody biomass. The mechanisms have been revised to describe the release pathway of K during the thermal treatment of annual biomass compiled from a review of the literature. K transformations may take place during both the devolatilization[1] and the char burnout stages,[1,14−16] primarily in the high temperature regime. Transformations between organic and inorganic K take place during the initial devolatilization, facilitating K release as the organic matrix is starting to decompose even at low temperatures.[14,17] At higher temperatures, KCl sublimation and K-silicate or aluminosilicate reactions are dominant during both devolatilization and char burnout, depending on the availability of Si, Cl, and divalent cations: Ca and Mg.[14,16,18−20] The possible release pathways during the char burnout also include the high temperature dissociation of carbonates, sulfates, and silicates, mentioned in decreasing order of significance.[16,21,22]

The primary alkali release to the gas phase has been found to begin at temperatures approaching 700 °C, enabling KCl sublimation.[1−3,14,16,17,21,23,24] Only a limited release of K (<10 wt %) has been observed at temperatures below 600−700 °C.[1,16] The low temperature release of K is thought to be related to the thermal decomposition of the organic structure,[14] for example, during the decomposition of alkaline carboxylates at approximately 300 °C or of phenol-associated K at around 400 °C.[14] A slower release of K has, however, been observed during pyrolysis, a phenomena thought to be caused by a higher diffusional resistance due to the still intact organic matrix.[1] The net

Received: July 25, 2011
Revised: September 26, 2011

   dx.doi.org/10.1021/ef201098n | *Energy Fuels* XXXX, XXX, 000–000

Table 1. Approximate Values for Different Types of Solid Fuels[44]

		wheat		wood chips		coal[a]		
species	unit	typical	variation	typical	variation	typical	variation	corn stover
moisture	wt %	14	8−23	45	20−60	3	2.1−14	12.82[b]
ash	wt %, dry	4.5	2−7	1.0	0.3−6	10	4−11	9.52[c]
volatiles	wt %, dry	78	75−81	81	70−85	30	5−35	72.68[d]
H	wt %, dry	5.9	5.4−6.4	5.8	5.2−6.1	5	3−6	5.68
C		47.5	47−48	50	49−52	88	69−93	45.39
N		0.7	0.3−1.5	0.3	0.1−0.7	1.5	1−1.8	0.57
S		0.15	0.1−0.2	0.05	<0.1	1	0.9−5	0.07
Cl		0.4	0.1−1.1	0.02	<0.1		0.04−0.17	0.69
Si		0.8	0.1−1.5	0.1	<1.0	2.10		2.4
Al		0.005	<0.03	0.015	<0.1	0.28		0.28
Fe		0.01	<0.03	0.015	<0.1		0.08−0.74	0.097
Ca		0.4	0.2−0.5	0.2	0.1−0.9		0.62−0.95	0.24
Mg		0.07	0.04−0.13	0.04	<0.1		0.57−0.78	0.13
Na		0.05	<0.3	0.015	<0.1		1.52−1.86	0.10
K		1.0	0.2−1.9	0.1	0.05−0.4		0.02−0.03	1.24
P		0.08	0.03−0.2	0.02	<0.1			0.062

[a] Data collected from separate source[2,43] compared to Spanish corn stover. [b] EN 14774-1:2009. [c] DS/EN 14775:2009. [d] DS/EN 15148:2009.

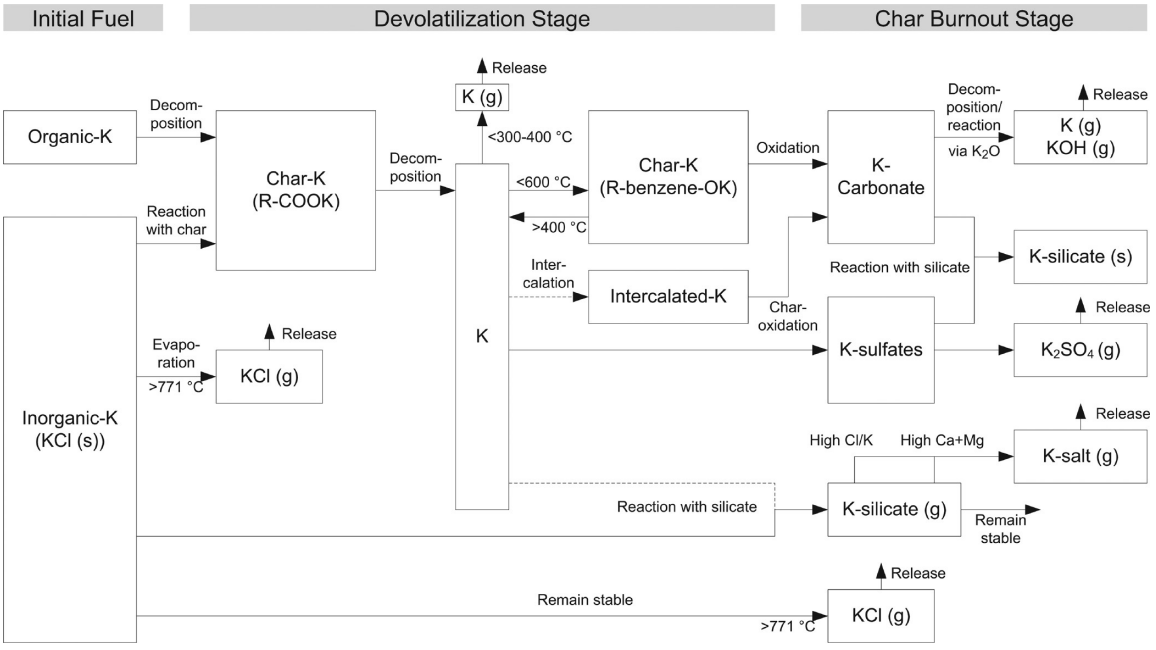

Figure 1. Possible reaction paths and release mechanisms of K during devolatilization and combustion, with special emphasis on the combustion of annual crops.

release of K at low to moderate temperatures may also be influenced by intercalation to the existing organic matrix.[21,25]

Silicates and aluminosilicates have shown great affinity toward K, binding it in an inorganic structure retained in the ash.[14,16,18,21,26−29] Such retention reactions will only take effect toward the final stages of the char burnout, as the organic matrix collapses, bringing the Si and K into closer contact.[16,18,21] The retention of K is inhibited by intercalation of other cations, especially Ca, being present to a great extent in the cell walls of plant material.[30] In addition, data from equilibrium studies and controlled release experiments have contributed to an increased understanding of the stability and behavior of released species.[5,21]

Chlorine Release Path. The release of Cl-associated species during combustion is the main cause of the induced active corrosion in the grate combustion of biomass.[2,5,13] In addition, Cl is known to facilitate the release of K, causing fouling problems upon condensation.[31]

Figure 2 summarizes pathways for Cl release during biomass combustion. The scheme is based on work conducted on release of inorganic matter from woody biomass,[3] and it was modified to include pathways relevant to the thermal conversion of annual

dx.doi.org/10.1021/ef201098n |*Energy Fuels* XXXX, XXX, 000–000

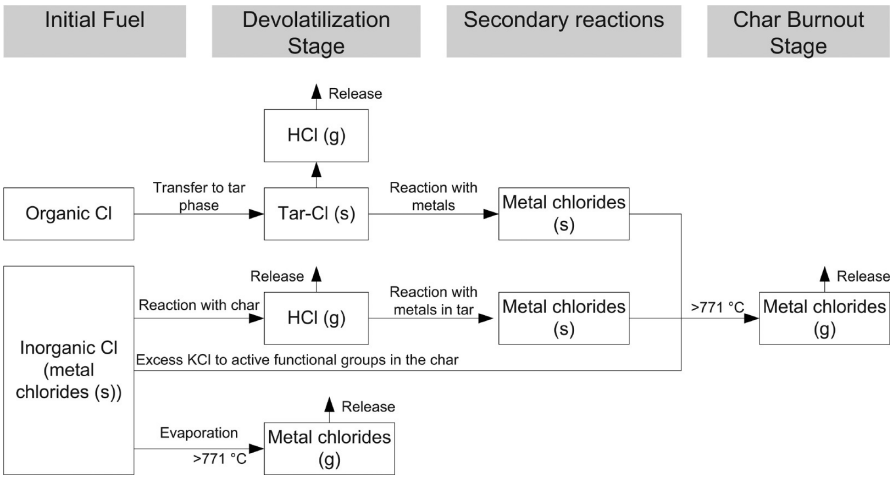

Figure 2. Possible reaction paths and release mechanisms of Cl during devolatilization and combustion, with special emphasis on combustion of annual crops.

biomass material. Cl release in the devolatilization stage takes place from both the organic and inorganic fraction of the Cl available in the fuel.[1,14,16,21,32] Chlorine release at low temperature in the form of tar associated Cl[33−37] or HCl[13,14,16,21,38] may possibly be recaptured in the char by secondary reactions with available metals.[1,39] High temperature KCl sublimation takes place during both pyrolysis and combustion,[1] potentially rereleasing recaptured Cl. Hence, a high volatilization of Cl will be expected.

All Cl species relevant in combustion chemistry are highly volatile.[1] The dominant Cl species found in biomass material is KCl, which remains stable in the solid phase until temperatures of approximately 700−800 °C. This is confirmed by SEM-EDX (scanning electron microscopy-energy dispersive X-ray spectroscopy) studies[1,3,39] and supported by thermodynamic calculations,[5,21] showing preferential bonding between Cl and K in the solid and gaseous phase. Hence, the release behavior and mechanisms of both K and Cl are highly dependent on the initial molar ratio between the two components.[16]

Contrary to K, low temperature release of Cl is commonly reported in the literature.[31] At temperatures as low as 300−400 °C, high levels (20−50%) of Cl release have been detected.[31] At these temperatures, the vapor pressure of KCl is negligible. However, because Cl initially is present as KCl,[40] it allows for ion-exchange reactions with functional groups in the organic matrix, such as[14]

$$\mathrm{R-COOH(s)} + \mathrm{KCl(s)} \rightarrow \mathrm{R-COOK(s)} + \mathrm{HCl(g)} \quad (1)$$

The release of Cl through reaction 1 is limited by the number of suitable functional groups in the organic matrix. At higher temperatures, alkali chlorides may react with the silica or alumina phases in the plant skeleton or in the external soil. SEM-EDX and thermodynamic modeling have shown how especially aluminosilicates are highly reactive toward the incorporation of alkali metals:[16,21,28,29,41]

$$2\mathrm{NaCl(g,l)} + \mathrm{H_2O(g)} + x\mathrm{Y(s)} \leftrightarrow \mathrm{Na_2O}\cdot x\mathrm{Y(s,l)} + 2\mathrm{HCl(g)} \quad (2)$$

where Y(s) signifies either a pure silica phase,[19] a pure alumina phase,[19] or combinations hereof.[19,20] At moderate temperatures, reaction 2 is kinetically limited,[19,20] and the competition from alkali chloride evaporation at temperatures exceeding 700 °C is significant. Hence, a two step release mechanism is observed for Cl: an initial low temperature release dominated by reaction 1, and a high temperature release primarily facilitated by the sublimation of alkali chlorides.[16,24,31]

During char burnout, the organic structure disintegrates, bringing the silicates in the outer structure of the biomass[30] into closer contact with retained K and Ca, primarily hosted in the center matrix of an organic structure.[16,18,21] Metal-silicate or metal-aluminosilicate reactions may then enhance the release of Cl, as K prefers association with the ash phase over chlorides.[19,20]

Sulfur Release Path. S is a macronutrient for plants that is partly metabolized and partly used in its ionic form. The S is absorbed from the soil through the roots, typically in the form of sulfates; from the roots, it is transported up the stem of the plant. Upon reaching the leaves of the plant, a gradual reduction takes place, resulting in the incorporation of S into the organic structure of the plant via the transformation into the basic amino acids cysteine and methionine, from which plant protein is synthesized:[18]

$$\text{sulfate} \rightarrow \text{sulfite} \rightarrow \text{sulfide} \rightarrow \text{cysteine} \rightarrow \text{protein synthesis} \quad (3)$$

The long migration of S, from uptake to reduction, results in a wide variety of S compounds in oxidation states ranging from (−II) to (+VI). Leaching experiments[40,42] suggest that organically associated S makes up approximately 50 wt % of the total S content. Excess sulfate in the soil, such as overconsumption of fertilizer, is absorbed by the plant roots and either stored as sulfate esters or emitted as a reduced form, such as H_2S.[30] This implies that great amounts of sulfates may be present in annual crops exposed to large amounts of fertilizer.

As a consequence of the division between organically and inorganically associated S, a two step release mechanism for S can be observed. The organically associated S is released at low temperatures, while inorganic S is retained in the ash until the combustion temperatures exceed approximately 900 °C.[14,16,24] No studies have, to the authors' knowledge, experimentally determined the temperature for the onset of the S release. We presume it to take place around 200 °C, as this agrees with the

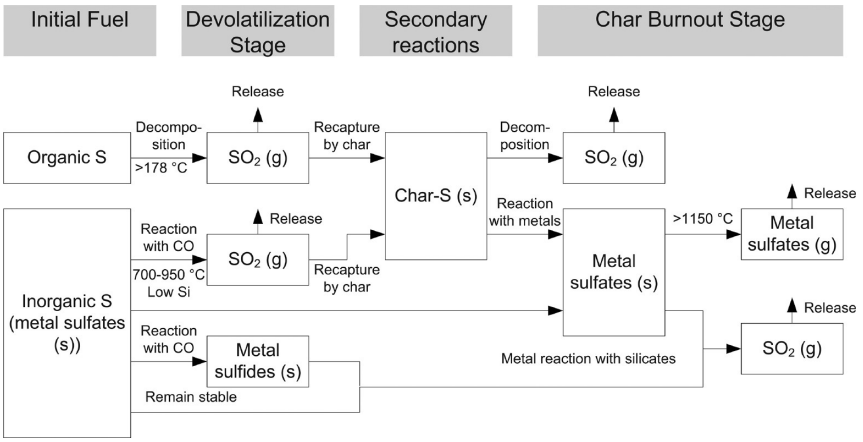

Figure 3. Possible reaction paths and release mechanisms of S during devolatilization and combustion with special emphasis on combustion of annual.

decomposition temperature of cystein (178 °C) and methionine (183 °C), the two main S-containing precursors for plant protein.[42] As seen in Figure 3, the S transformations are complex and include both low and high temperature release, as well as secondary capture to the char bed. The main product of S release is SO_2. Reduced species of S are dominant in the devolatilization stage, while S species in higher oxidation stages are more profound during the char burnout.[18] Thermodynamic equilibrium calculations have shown how only reduced forms of S may form stable compounds under the reducing conditions of the pyrolysis stage.[18] This suggests that it is possible for sulfatic S to transform through reductive decomposition by interactions with organic material.[43] The second release step occurs during the char burnout stage where S may be present in higher oxidation states.[18] Pathways include the evaporation of alkali sulfates at temperatures above 1000 °C or the decomposition of sulfate, releasing SO_2 to the gas phase, while the cation is incorporated into the silicate melt.

The balance between organic and inorganic S species is important for the release behavior. The two types of S are primarily relevant in different temperature regions and, thereby, different stages in the combustion process. S released during the devolatilization can be recaptured into the fuel bed following secondary reactions with the char matrix. Subsequently it will be rereleased during the char burnout stage alongside the high temperature inorganic release of S compounds.

EXPERIMENTAL SECTION

In the present work, the release characteristics of the inorganic matter have been investigated by thermal treatment and subsequent char or ash analysis of the corn stover residues in a laboratory sized rig, with temperature and flow control. The setup has been used in earlier work to characterize release behavior of woody and annual biomass,[1,3] and only a brief description is given here.

The reactor setup consists of a ceramic tube with an inner diameter of 50 mm placed horizontally in a dual zone electric oven directly connected to a neighboring water-cooled chamber for efficient quenching of the reacted samples.

The gas mixture in the primary air is controlled by individual mass flow controllers, regulating the flow of O_2 and N_2 for both the primary and secondary (burnout) air supply. The sample is introduced to the oven in a Pt/Au boat (110 × 30 × 18 mm) with a perforated lid on top to avoid particle entrainment.

The reaction progress is followed by a series of gas analyzers continuously monitoring the O_2, CO, and CO_2 levels in the exhaust, with a standard deviation of ±1.7%. A reaction stage is considered to be complete when the CO and CO_2 levels drop below 40 and 50 ppm, respectively, constituting the respective detection limits of the gas analyzers. During the experiments, CO and CO_2 concentrations reach values of 16 and 10 vol %.

A typical experiment (both pyrolysis and combustion) included approximately 2.6 g of corn stover, filling the sample boat without compressing the fuel bed. The sample boat was placed in the water cooled chamber connected directly to the reactor. After sealing the system, the setup was purged with 4 normal liter^{STP}/min (NL/min) of N_2 through the primary air inlet. During all stages of the experiment, a flow of 2 NL/min 21 vol % O_2 in N_2 gas mixture was added through the secondary air inlet to fully oxidize any uncombusted volatiles. Insertion of the sample was carried out by pushing the sample boat with a metal rod. The insertion process was completed in less than 10 s and resulted in initial heating rates of 5−40 °C/s, registered by the thermocouple positioned in the middle of the sample boat.

For pyrolysis experiments, the flow of 4 NL/min of N_2 was maintained through the primary inlet until the experiment was terminated. For the combustion experiments, devolatilization in N_2 was first achieved until devolatilization products were no longer detected in the flue gas. Hereafter, the O_2 level in the primary air was progressively increased, 2 → 5 → 10 → 21 vol % (maintaining a total primary flow of 4 NL/min), to minimize the temperature overshoot caused by the heat of reaction. In this way, only small fluctuations in the fuel bed temperature were observed (<20 °C). However, it should be kept in mind that the temperature probe is not able to measure the surface temperature of the fuel itself.

After the complete reaction, the sample was retracted to the water cooled chamber and cooled to room temperature under constant N_2 purge before the reactor was opened and the sample weighted and stored. After weighing and ash collection, the sample vessel was rinsed with ultrapure water to collect any salts deposited in the vessel. The rinsing water was weighed and stored for later analysis. The rinsing water of a selected sample was analyzed for Ca, K, Na, Cl, and SO_4, but only insignificant amounts were observed, and it was therefore decided to exclude them from the result processing.

The char and ash samples were analyzed by DONG Energy Power A/S at Enstedværket, Denmark. The contents of Ca, K, Mg, Na, P, and Si were prepared by pressure decomposition in acid and detected by inductively coupled plasma-optical emission spectroscopy (ICP-OES, standard: CEN/TS 15290, 2006), while S and Cl were detected by ion chromatography (IC, standard: CEN/TS 15289, 2006).

The corn stover fuel has been characterized according to Danish and European standards by ultimate and proximate analysis (Table 1).

dx.doi.org/10.1021/ef201098n |Energy Fuels XXXX, XXX, 000–000

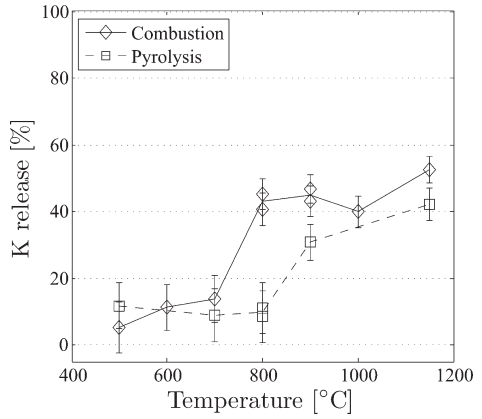

Figure 4. Comparison of K release during pyrolysis and combustion, respectively, in the 500−1150 °C temperature range.

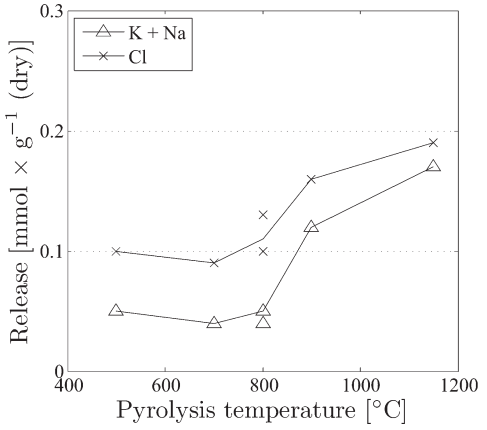

Figure 5. Absolute release of key inorganic species in [mmol g^{-1}] of dry biomass during devolatilization.

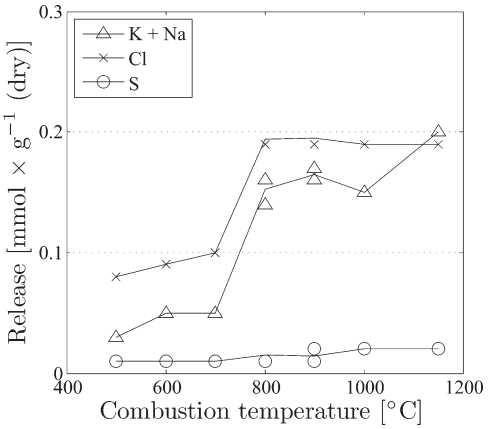

Figure 6. Absolute release of key inorganic species in [mmol g^{-1}] of dry biomass during combustion.

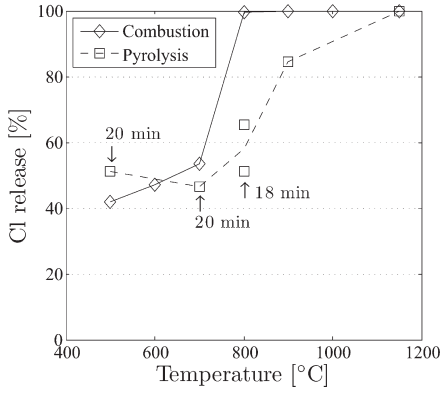

Figure 7. Relative Cl release during pyrolysis and combustion in the temperature range 500−1150 °C. The devolatilization time is 15 min unless otherwise stated.

Preliminary analyses of the fuel at VTT, Finland, indicated a strongly varying ash content (up until ∼40 wt %). A low content of carbon suggests that a large fraction of the ash originates from soil gathered during harvesting. Thus, thorough sieving of the fuel on a 1 mm wire mesh was done to remove soil prior to analysis and experiments.

RESULTS

The results section consists of three parts: (1) release experiments, (2) char and ash samples, and (3) thermodynamic equilibrium calculations. The release experiments yield data for the pyrolysis and combustion processes. On the basis of the elemental analysis of the char and ash samples, release profiles are constructed for K, Cl, and S.

Release Experiments. *Potassium Release.* The release of K during devolatilization and char burnout is presented on a relative basis in Figure 4. Only low levels (5−10%) of K are released below 700 °C. Under combustion conditions between 700 and 800 °C, a significant increase in K release is observed. Under pyrolysis conditions, this high temperature release is shifted approximately 100 °C toward higher temperatures.

The release of alkali metals and Cl is closely related, as will be explained in the following sections on the SEM-EDX and the equilibrium calculations. The comparison of the absolute release (cf. Figures 5 and 6) of K, Na, and Cl shows good correlation between the rates at which the cationic and anionic species are released during pyrolysis and combustion, respectively. The relatively low S release of the fuel (Figure 6) indicates little release of alkali species through sulfatic species.

Chlorine Release. The relative release of Cl is presented in Figure 7 for both combustion and pyrolysis experiments. Around 50 wt % of the Cl is released at temperatures below 700 °C, with an onset of release below 500 °C, regardless of the combustion stage. Increasing the combustion temperature to 800 °C results in complete dechlorination. Under pyrolysis conditions, complete dechlorination is shifted toward higher temperatures. The low temperature release of Cl agrees with similar observations in the literature.[31] The onset (700−800 °C) of the high temperature release also corresponds to findings in the literature,[1,3,16,24] quickly reaching complete dechlorination.

Sulfur Release. Significant differences in the observed release of S have been observed during pyrolysis and combustion, respectively (cf. Figure 8). A low temperature release of approximately 60 wt % is observed at temperatures below 500 °C, regardless of the combustion stage. Under pyrolysis conditions, no further release is observed as the reaction temperature is increased. At combustion conditions, an additional S release is seen around 900 °C, increasing progressively until reaching complete desulfurization at 1150 °C.

Char and Ash Samples. The present section, as well as the following section on thermodynamic equilibrium calculations,

dx.doi.org/10.1021/ef201098n |*Energy Fuels* XXXX, XXX, 000–000

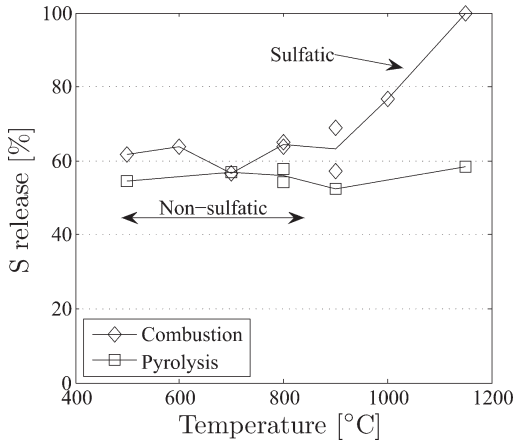

Figure 8. Comparison of the relative S release at pyrolysis and combustion conditions.

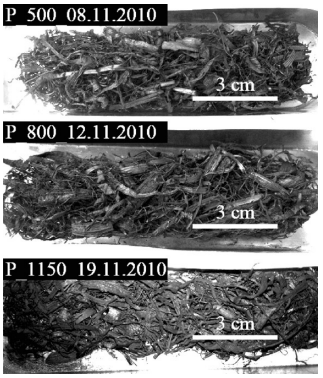

Figure 9. Corn stover char samples after devolatilization at 500 (top), 800 (middle), and 1150 °C (bottom).

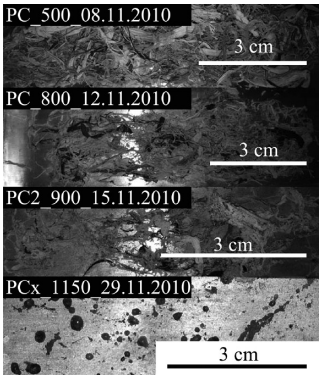

Figure 10. Fuel samples after complete combustion at 500 (top), 800 (middle top), 900 (middle-bottom), and 1150 °C (bottom).

aims to support the findings and hypotheses presented on the basis of the release experiments. It includes investigations of the changes in the physical structure by SEM imaging combined with EDX.

Figures 9 and 10 show pictures of selected samples, representing the full temperature range, after pyrolysis and combustion, respectively. No significant changes occur to the physical structure of the fuel during pyrolysis. After pyrolyzing at 1150 °C,

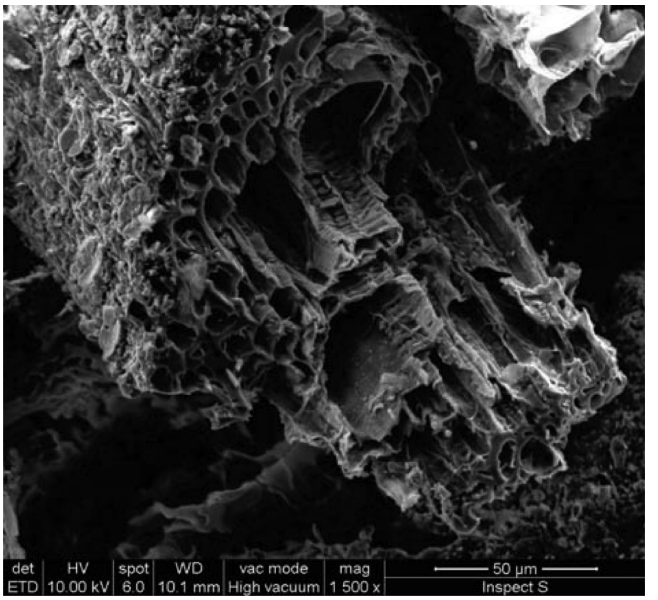

Figure 11. SEM image of a corn stover sample devolatilized at 500 °C for 20 min.

a slight collapse of the char bed is visible. The fraction of volatiles is found to increase linearly with the pyrolysis temperature, going from ∼72 wt % of volatile matter on a dry basis at 500 °C (20 min) to almost 80 wt % at 1150 °C (15 min). The proximate analysis yields a slightly lower fraction of volatile material than the sample from the experimental setup at corresponding temperatures. This is possibly due to soil contamination, as indicated by a slightly higher ash fraction.

Contrary to the devolatilized samples, the combusted samples undergo significant changes, detectable by the naked eye (cf. Figure 10), as the reaction temperature is increased. The bed of ash gets denser as the reaction temperature is increased from 500 through 900 °C; however, the overall fibrous structure is maintained. At 1150 °C, the sample has completely agglomerated into large clusters of melted ash.

SEM images of the samples yield further insight into the changes in the char and ash morphology. Figures 11 and 12 illustrate the structural changes when increasing the devolatilization temperature from 500 (20 min) to 1150 °C (15 min). At 500 °C, the stemlike structure is easily recognizable with clearly defined channels. At 1150 °C, some deterioration of the stem structure can be seen; however, cell walls are still found to be intact toward the center of the stem. These physical changes take place at elevated temperatures, that is, >800 °C, as no significant differences in the structure have been observed by SEM imaging when increasing the reaction temperature from 500 to 800 °C. The preservation of the plant skeleton shape implies a limited global chemical availability due to physical constraints, preventing elements of different locations to freely associate. As such, diffusional resistance can be expected to be of significance throughout the entire pyrolysis stage.

SEM images of ash samples have likewise been obtained, showing significant structural changes as the combustion temperature is increased from 500 to 1150 °C, in agreement with Figure 10. At 500 °C, stemlike structures may still be identified. Small clusters of KCl are observed by EDX analysis on the surface of these relatively large particles, in accordance with the low K

dx.doi.org/10.1021/ef201098n |*Energy Fuels* XXXX, XXX, 000–000

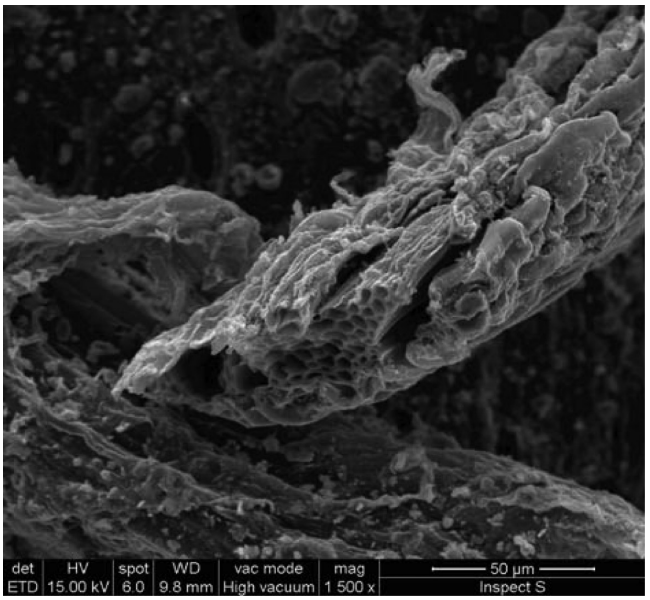

Figure 12. SEM image of a corn stover sample devolatilized at 1150 °C for 15 min.

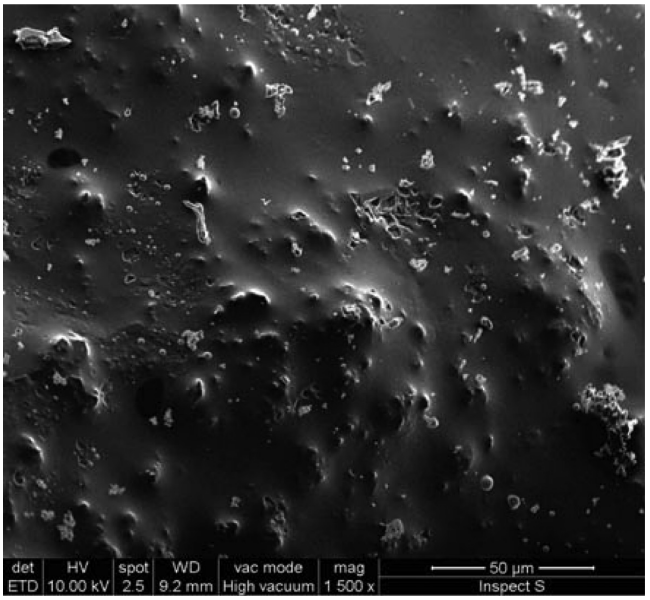

Figure 13. SEM picture of corn stover pyrolyzed and combusted at 1150 °C. Large agglomerates with a dense and closed structure dominate the sample.

release during pyrolysis and combustion; see Figure 4. At 700 °C, two types of particles are identified: a fibrous structure rich in Si with discrete particles of almost pure KCl and a more meltlike structure rich in Al and Si. This marks the transition from a rigid and porous structure to an ash melt. At 1150 °C, most of the particles have agglomerated into large structures, as can be seen in Figure 10. The surfaces of these agglomerates are smooth and closed, as illustrated in Figure 13, consisting mainly of aluminosilicates. The surface is sprinkled with small grains, containing slightly higher levels of K and Ca than the background.

Thermodynamic Equilibrium Calculations. Global equilibrium calculations are useful to gain information on species stability

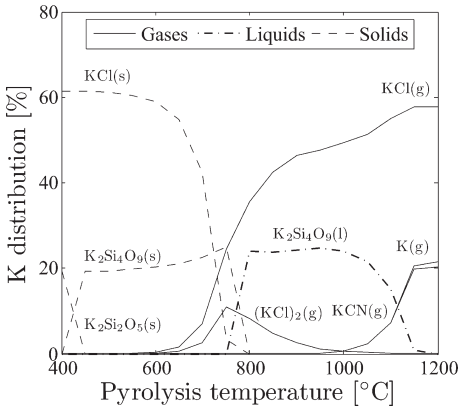

Figure 14. Calculated K distribution under reducing conditions.

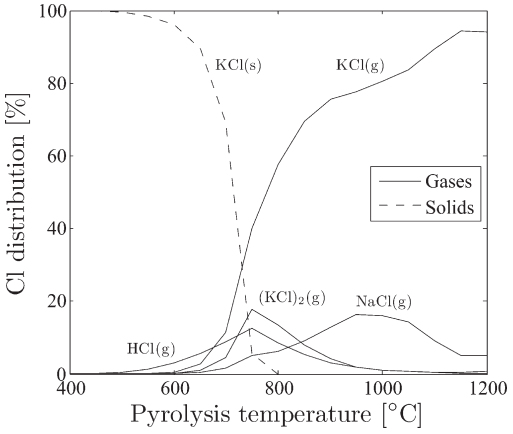

Figure 15. Calculated Cl distribution under reducing conditions.

and phase distribution.[1−3,5,21] The thermodynamic models used are based on the Gibbs free energy minimization of a predefined mass balance constrained system as function of temperature. The models rely on an assumption of complete accessibility, that is, ideal mixing, of all components; this is unlikely, considering the complexity of the system. Thus, the aim of the thermodynamic equilibrium calculations will be to qualitatively confirm trends rather than to quantify species and distributions.

The equilibrium calculations are carried out using the FactSage (version 6.0) simulator. This program calculates the equilibrium composition fed with the molar composition of the fuel based in Table 1, including only H, C, O, Si, N, K, Cl, Ca, Mg, Na, S, and P in order to reduce the number of possible species.

Reducing Conditions. The prediction of potentially stable phases of especially alkali and Cl-containing species during the reducing conditions of the devolatilization stage is of interest as a significant release of both alkali and halogen material may take place during the pyrolysis.[1,13,16,21,31,14,38] Figures 14 and 15 show the equilibrium distributions of K and Cl, respectively.

As expected,[40,45,46] a close association between K and Cl is favored across the total temperature range. Potentially 100% of the Cl is present in the form of solid KCl at temperatures below 600 °C. The sublimation of KCl is predicted to be the dominate release mechanism for both K and Cl, in agreement with the negligible K release observed at low temperatures (cf. Figure 4). The release of Cl as HCl is predicted to begin at lower temperatures than that for the evaporation of KCl. This corresponds

dx.doi.org/10.1021/ef201098n |*Energy Fuels* XXXX, XXX, 000–000

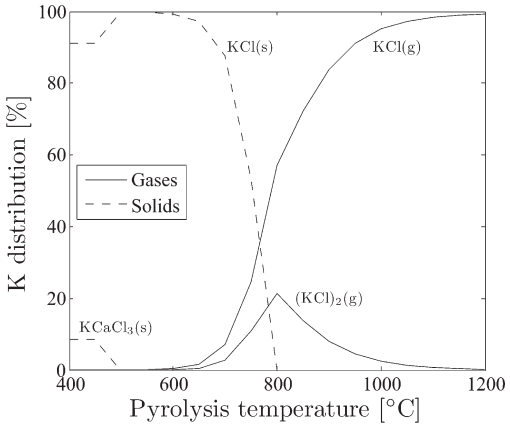

Figure 16. Calculated K distribution under reducing conditions. Cl/K = 5.5.

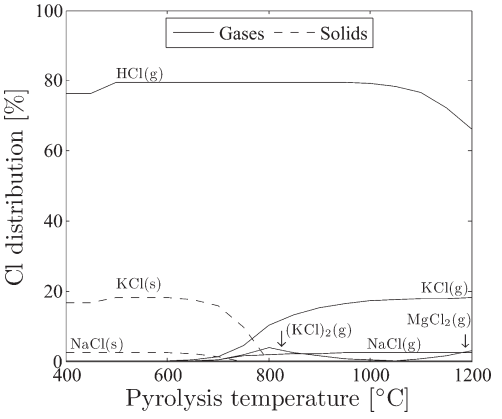

Figure 17. Calculated Cl distribution under reducing conditions. Cl/K = 5.5.

well to earlier observations in the literature,[16,31] reporting an early Cl release at temperatures below 300 °C, too low to be caused by KCl evaporation.[47]

Figure 14, describing the K distribution, shows how the high temperature release of K in the form of KCl is equivalent to the available amount of total Cl in the feedstock fuel. The simulation indicates a high temperature release of elemental K to the gas phase. Such a release could occur through the following reaction:[16]

$$K_2O(SiO_2)_n(s,l) + H_2O(g) \rightarrow 2KOH(g) + nSiO_2(s) \quad (4)$$

The residual K is favored as part of a K-silicate melt at temperatures exceeding 800 °C. This apparent K-retention effect will be discussed further later on. Additional simulations with increased Cl (in excess to K) result in complete devolatilization of K species, primarily in the form of KCl, as seen in Figure 16. The Cl in excess to K is released in the form of HCl across the entire temperature range (400−1200 °C) as seen in Figure 17.

Common for all simulations under reducing conditions is that only reduced forms of S are stabilized, regardless of the phase. This is in good agreement with other equilibrium calculations performed on similar annual crops,[18] as well as the limited S release during pyrolysis, as observed in Figure 8.

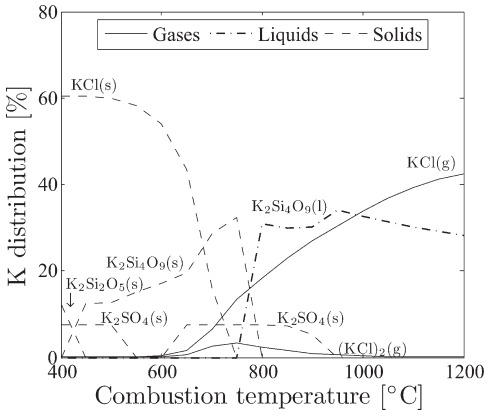

Figure 18. Calculated K distribution under oxidizing conditions.

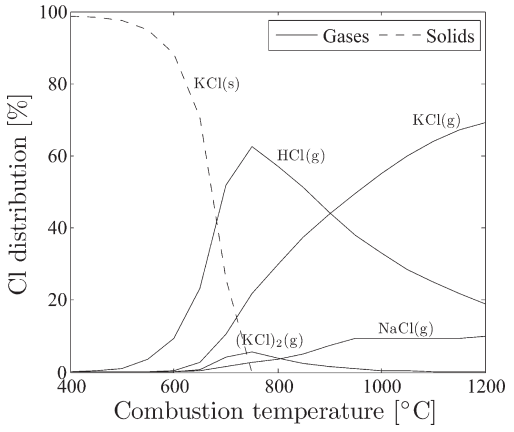

Figure 19. Calculated Cl distribution under oxidizing conditions.

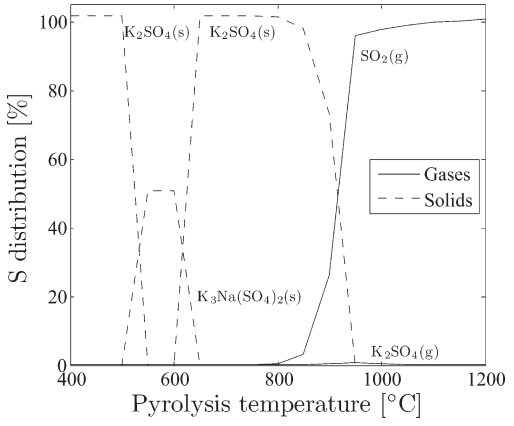

Figure 20. Calculated S distribution under oxidizing conditions.

Oxidizing Conditions. Simulations under oxidizing conditions are carried out with a primary air supply equivalent to 6 vol % O_2 in the exhaust. It can be seen through comparison of Figures 14 and 18 how the introduction of O_2 during the combustion is predicted to shift the release of gaseous K toward more elevated temperatures, while increasing the fraction of K-silicate.

This behavior is also reflected in the Cl distribution simulation, see Figure 19, where the contribution from the HCl formation is

dx.doi.org/10.1021/ef201098n |*Energy Fuels* XXXX, XXX, 000–000

Table 2. Molar Ratios Related to the Release and Retention of Key Inorganic Species in the Corn Stover Fuel

		Cl/K	K/Si	(Mg+Ca)/Si	q^a
corn stover	(mol/mol)	0.61	0.37	0.13	2.2

[a] q is the molar ratio of cation and anion forming elements: $q = (K + Na + 2(Ca + Mg))/(2S + Cl + 1.5P)$.

significant in order to compensate for the unavailability of K. The corresponding S simulations (Figure 20) indicate the stable phases of S under oxidizing conditions. The trend corresponds to the findings in the literature, suggesting a beginning decomposition of K_2SO_4 at around 900−1000 °C.[1]

DISCUSSION

Potassium Release. The release of K is found to take place primarily in connection to the sublimation of KCl at temperatures exceeding around 700 °C. A low (5−10 wt %) release has been observed at temperatures below 700 °C, where the vapor pressure of K salts is too low to make any significant contribution to the net release of K. The K released at low temperatures (<500 °C) is thought to be organically associated as, for example, carboxylates or phenols, decomposing at around 300 and 400 °C, respectively.[14]

The same release pattern is seen for both the pyrolysis and the combustion stages, leading us to conclude that K primarily is released as the first reaction front passes through the dried out bed in a moving grate facility. The release data from the lab-scale experiments (cf. Figure 4) could indicate that the release of K requires higher temperatures (around 100 °C) during the pyrolysis stage. Part of this phenomena could be explained by a higher effective reaction temperature during combustion due to the local heat generated from the combustion process, thus, increasing the vapor pressure and convective flux of KCl under combustion conditions. However, the delayed release could also be caused by a higher diffusional resistance during devolatilization, caused by the still intact organic matrix; see Figures 11 and 12. Finally, a lower residence time (15−20 min during pyrolysis versus 54−110 min during combustion) may contribute to the difference. Supporting the latter, Knudsen et al.[16] reported that longer reaction times lead to increases in K volatilization during pyrolysis.

The correlation between the absolute release of alkali material and Cl (see Figures 5 and 6) supports the thermodynamic equilibrium calculations, indicating that K primarily will associate with Cl, with an onset of sublimation at around 700 °C (cf. Figures 14 and 18). The quantity of alkali material released seems to be limited by the Cl availability for salt formation, given that K originally is present in stoichiometric excess to Cl (cf. Table 2). The release of K will cease as the fuel, undergoing pyrolysis or combustion, reaches a state of complete dechlorination. This behavior is evident when considering the release profiles of K and Cl. High temperature release of K after complete dechlorination is thought to be governed by the thermal decomposition of carbonates,[16] leading to the release of K or KOH to the gas phase, depending on the partial pressure of water vapor in the reaction gas. However, for corn stover, the carbonate dissociation pathway is competing with the incorporation of K to a ceramic phase. As a supplier of excess Si, the external soil may play a role in the retention mechanism of K. However, this needs to be verified experimentally. It is expected that external soil only has limited influence on the plant associated elements due to physical constraints[30] and kinetic limitations at low temperatures. However, as K incorporation in the silicate phase is not relevant until temperatures exceeding 800 °C, this could be explained by an advanced level of disintegration of the plant structure, as well as the introduction of melted phases, increasing diffusional transport significantly.

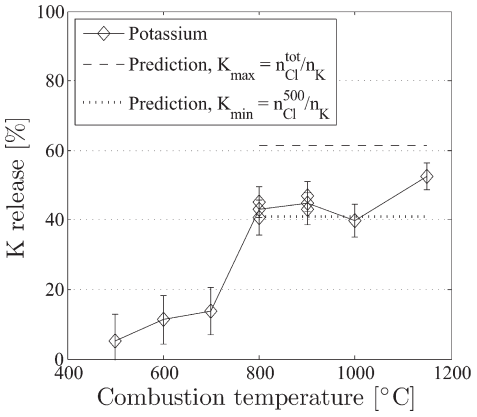

Figure 21. K release predictions based on (- - -) the initial Cl content and (···) the Cl content after the low temperature Cl release, both relative to the initial K concentration. The predicted release is compared to the relative K release profile.

Table 2 summarizes the molar ratios of key elements regarding the retention properties of the ash phase. The K/Si-ratio signifies an estimate of the alkali retention capacity, as the thermodynamic models show a significant leverage of Si-containing alkali species in the solid phase at elevated temperatures. The (Mg + Ca)/Si ratio indicates the significance of competing reactions for cationic incorporation to the silicate phase. The q ratio indicates the overall molar ratio between cation and anion forming elements, constructed under the assumptions that S is solely present as SO_4^{2-}, P is assumed to be present in an equimolar mixture of $H_2PO_4^-$ and HPO_4^{2-}, and N is completely omitted, presuming the majority of the total quantity of N will be organically associated.[30]

Taking the ash phase chemistry into account leads to a simple method to estimate the high temperature K release, on the basis of the experimental data from the controlled release experiment and subsequent elemental analysis:

$$K_{release}^{>800} = \frac{n_{Cl}^{500}}{n_K} 100\% \quad (5)$$

where n_{Cl}^{500} is the molar quantity of Cl available at 500 °C and n_K is the initial molar quantity of K. The application of eq 5 to the ash analysis results from the experimental series is shown in Figure 21 depicting the K release profile under combustion conditions, as well as the predicted high temperature K release with and without an initial low temperature release of Cl, K_{max} and K_{min}, respectively. When correcting for the initial release of Cl, n_{Cl}^{500}, one finds a good correspondence between the predicted high temperature K release, K_{min}, and the release profile achieved by the controlled release experiments.

Chlorine Release. As explained in the preceding section, the K and Cl releases during thermal treatment of biomass fuels are closely related. Cl is thought to be the main facilitator for K release; thus, predicting the Cl release is essential to estimate the high temperature K release (cf. eq 5).

dx.doi.org/10.1021/ef201098n |*Energy Fuels* XXXX, XXX, 000–000

The Cl release profiles suggest a two step release mechanism: low and high temperature releases, respectively. The low temperature release begins at temperatures below 500 °C and accounts for approximately 40−50 wt % of the feedstock Cl content during both pyrolysis and combustion. The relevant temperature range for the low temperature release does not fit with the evaporation of any of the Cl-containing compounds (mainly KCl) predicted by the thermodynamic equilibrium calculations. Hence, the initial Cl release is thought to be governed by ion-exchange mechanisms, such as the interaction of KCl and carboxylic groups in the organic matrix, forming gaseous HCl and an alkaline carboxylate, following reaction 6:

$$\mathrm{R-COOH(s)} + \mathrm{KCl(s)} \rightarrow \mathrm{R-COOK(s)} + \mathrm{HCl(g)} \quad (6)$$

Alternatively, at more elevated temperatures, by the incorporation of alkali metals to the silicate phase under the subsequent release of HCl given in reaction 7:

$$2\mathrm{NaCl(g,l)} + \mathrm{H_2O(g)} + x\mathrm{Y(s)} \leftrightarrow \mathrm{Na_2O}\cdot x\mathrm{Y(s,l)} + 2\mathrm{HCl(g)} \quad (7)$$

Through reaction 6, it is clear how only a finite quantity of Cl may be released, limited by the number of available functional groups. Assuming that all chloride precipitates as KCl upon drying, the average low temperature release of Cl may be estimated from the controlled release experiments. Analytical proof for the assumed predominant association between K and Cl after a completed drying process has, to the authors' knowledge, not been reported in the literature. However, ionic associations are indicated by the leaching experiment, removing more than 95% of both K and Cl.

An average low-temperature (≤700 °C) Cl release during both pyrolysis and combustion of $94 \pm 8.8\ \mu\mathrm{mol}\ g_{\mathrm{fuel}}^{-1}$ (dry basis) has been observed during the controlled release experiments. Hence, the extent of reaction 6 may be estimated, assuming that the fuel samples used for the controlled release experiments are representative. It should be noticed that the value is highly fuel specific. However, the initial concentration of Cl in the fuel has been shown to be highly sensitive to both use of fertilizer[44,48] and natural leaching on the field before collection.[31,44,49,50] Hence, it is not possible to quantify the fraction of Cl available for reaction through reaction 6 on a percentage basis of the initial Cl.

All relevant metal chlorides in the system are highly volatile, which is why high temperature treatment of biomass presumably will cause complete dechlorination. The rate at which Cl leaves the fuel may be estimated from evaporation models of primarily KCl[1] combined with suitable diffusional models. However, as combustion normally takes place at temperatures significantly exceeding 700−800 °C, such models are commonly considered redundant.

Sulfur Release. The differences in release characteristics of S, illustrated in Figure 8, can be attributed to the two types of S associations in the biomass fuel. The constant level of ∼60% of released S observed during the pyrolysis is consistent with the release of organically bound S. In this way, the initial S release is expected to begin as the organic structure starts to decompose. The fact that further S release is independent of temperature indicates that the high temperature release is chemically restricted rather than mass transfer limited. Such a chemical constraint corresponds well to the expected approximate 50/50 distribution between organically and inorganically associated S. Hence, the initial low temperature S release may be estimated by chemical fractionation, determining the ratio between organically associated S and S in solution.

The high temperature S release during the char burnout phase (combustion conditions) is thought to be caused by the evaporation or dissociation of alkali sulfates or sulfate decomposition to SO_2 as alkali species are incorporated into the silicate ash phase. However, the absolute amount of S compared to that of alkali species in the corn stover (cf. Table 1) is too low to yield conclusive tendencies in the alkali release profiles. Hence, it can only be assumed that S is released, to some extent accompanied by alkali metals, and, therefore, possibly contributes, however insignificantly, to the high temperature alkali release occurring after complete dechlorination (cf. Figure 6).

Knudsen et al.[16] found a good correlation between the high temperature relative S release and the combustion temperature. By linear regression, he derived a correlation equation averaged across the release data from three Si-rich fuels: barley, rice, and wheat.

Fitting a linear expression to the obtained release data yields a regression equation for the high temperature S release from corn stover:

$$\%\mathrm{S\ release} = 0.10T - 22 \quad \text{for } T \in [800 : 1150°C] \quad R^2 = 0.80 \quad (8)$$

For corn stover, the fit only yields a coefficient of determination of $R^2 = 0.80$, compared to a $R^2 = 0.96$ found by Knudsen,[1] and it is doubtful whether this method of prediction is applicable for the corn stover fuel.

CONCLUSION

The release patterns of key inorganic species (K, Cl, and S) have been determined by means of char and ash analysis of corn stover fuel undergoing thermal treatment (500−1150 °C) under pyrolysis and combustion conditions, respectively.

Close correlation has been found between the release of K and Cl. The final high temperature K release seems to be limited by the quantity of available Cl. A significant low temperature Cl release further limits the availability for Cl facilitated K release at elevated temperatures. The ash phase has proven efficient in retaining K not released as KCl.

S is released through a two step release mechanism related to the organic and inorganic fraction of S, respectively. Organic S is released at low temperatures regardless of combustion stage, while inorganic S is only observed to leave at elevated temperatures under combustion conditions.

AUTHOR INFORMATION

Corresponding Author

*Phone: +45 45 25 28 40. Fax: +45 45 88 22 58. E-mail: PGL@kt.dtu.dk.

ACKNOWLEDGMENT

Funding from EU Contract No. 23946 "Demonstration of a 16 MW High Energy Efficient Corn Stover Biomass Power Plant" is gratefully acknowledged, as well as the fuel delivery by Acciona Energia and fuel preparation by VTT, Finland.

REFERENCES

(1) Knudsen, J. N. *Volatilization of Inorganic Matter during Combustion of Annual Biomass*, Ph.D. thesis, Technical University of Denmark, Lyngby, Denmark, 2004; ISBN: 87-91435-11-0.

(2) Frandsen, F. J. *Ash Formation, Deposition and Corrosion When Utilizing Straw for Heat and Power Production*; Technical University of Denmark: Lyngby, Denmark, 2011; ISBN: 978-87-92481-40-5.

(3) van Lith, S. C. *Release of Inorganic Elements during Wood-Firing on a Grate*. Ph.D. thesis, Technical University of Denmark, Lyngby, Denmark, 2005; ISBN: 87-91435-29-3.

(4) Zhang, L.; Xu, C. C.; Champagne, P. *Energy Convers. Manage.* **2010**, *51*, 969–982.

(5) Michelsen, H. P.; Frandsen, F.; Dam-Johansen, K.; Larsen, O. H. *Fuel Process. Technol.* **1998**, *54*, 95–108.

(6) Miles, T. R.; M., T. R., Jr.; Baxter, L. L.; Bryers, R. D.; Jenkins, B. M.; Oden, L. L. *Biomass Bioenergy* **1996**, *10*, 125–138.

(7) Steinberg, M.; Schofield, K. *Symp. (Int.) Combust., [Proc.]* **1996**, *26*, 1835–1843.

(8) Bryers, R. W. *Prog. Energy Combust. Sci.* **1996**, *22*, 29–120.

(9) Durie, R. A.; Milne, J. W.; Smith, M. Y. *Combust. Flame* **1977**, *30*, 221–230.

(10) Grabke, H. J.; Reese, E.; Spiegel, M. *Corros. Sci.* **1995**, *37*, 1023–1043.

(11) Hansen, L. A.; Nielsen, H. P.; Frandsen, F. J.; Dam-Johansen, K.; Hørlyck, S.; Karlsson, A. *Fuel Process. Technol.* **2000**, *64*, 189–209.

(12) van Lith, S. C.; Frandsen, F. J.; Montgomery, M.; V., T.; Jensen, S. A. *Energy Fuels* **2009**, *23*, 3457–3468.

(13) Werther, J.; Saenger, M.; Hartge, E.-U.; Ogada, T.; Siagi, Z. *Prog. Energy Combust. Sci.* **2000**, *26*, 1–27.

(14) van Lith, S. C.; Jensen, P. A.; Frandsen, F. J.; Glarborg, P. *Energy Fuels* **2008**, *22*, 1598–1609.

(15) Novaković, A.; van Lith, S. C.; Frandsen, F. J.; Jensen, P. A.; Holgersen, L. B. *Energy Fuels* **2009**, *23*, 3423–3428.

(16) Knudsen, J. N.; Jensen, P. A.; Dam-Johansen, K. *Energy Fuels* **2004**, *5*, 1385–1399.

(17) Davidsson, K. O.; Stojkova, B. J.; Pettersson, J. B. C. *Energy Fuels* **2002**, *16*, 1033–1039.

(18) Knudsen, J. N.; Jensen, P. A.; Lin, W.; Frandsen, F. J.; Dam-Johansen, K. *Energy Fuels* **2004**, *18*, 810–819.

(19) Kyi, S.; Chadwick, B. L. *Fuel* **1999**, *78*, 845–855.

(20) Schümann, H.; Unterberger, S.; Hein, K. R. G.; Monkhouse, P. B.; Gottwald, U. *Faraday Discuss.* **2001**, *119*, 433–444.

(21) Jensen, P. A.; Frandsen, F. J.; Dam-Johansen, K.; Sander, B. *Energy Fuels* **2000**, *14*, 1280–1285.

(22) Dare, P.; Gifford, J.; Hooper, R. J.; Clemens, A. H.; Damiano, L. F.; Gong, D.; Matheson, T. W. *Biomass Bioenergy* **2001**, *21*, 277–287.

(23) Olsson, J. G.; Jäglid, U.; Petterson, J. B. C.; Hald, P. *Energy Fuels* **1997**, *11*, 779–784.

(24) van Lith, S. C.; V. Alonso-Ramírez, P. A. J.; Frandsen, F. J.; Glarborg, P. *Energy Fuels* **2006**, *20*, 964–978.

(25) Wornat, M. J.; Hurt, R. H.; Yang, N. Y. C.; Headley, T. J. *Combust. Flame* **1995**, *100*, 131–143.

(26) Steenari, B. M.; Lindqvist, O. *Biomass Bioenergy* **1998**, *14*, 67–76.

(27) Zheng, Y.; Jensen, P. A.; Jensen, A. D. *Fuel* **2008**, *87*, 3304–3312.

(28) Tran, K.-Q.; Iisa, K.; Steenari, B.-M.; Lindqvist, O. *Fuel* **2005**, *84*, 169–175.

(29) Punjak, W. A.; Uberoi, M.; Shadman, F. *AIChE J.* **1989**, *35*, 1186–1194.

(30) Marschner, H. *Marschner's Mineral Nutrition of Higher Plants*, 2nd ed.; Academic Press: San Diego, CA , 2002; ISBN: 0-12-473543-6.

(31) Björkman, E.; Strömberg, B. *Energy Fuels* **1997**, *11*, 1026–1032.

(32) Pedersen, A. J.; van Lith, S. C.; Frandsen, F. J.; Steinsen, S. D.; Holgersen, L. B. *Fuel Process. Technol.* **2010**, *91*, 1062–1072.

(33) Hamilton, J. T. G.; McRoberts, W. C.; Keppler, F.; Kalin, R. M.; Harper, D. B. *Science* **2003**, *301*, 206–209.

(34) Egsgaard, H.; Ahrenfeldt, J.; Henriksen, J.; B., U. *18th European Biomass Conference and Exhibition* 2010, 590−592.

(35) Palmer, T. Y. *Nature* **1976**, *263*, 44–46.

(36) Eklund, G.; Pedersen, J. R.; Strömberg, B. *Chemosphere* **1987**, *16*, 161–166.

(37) Eklund, G.; Pedersen, J. R.; Strömberg, B. *Chemosphere* **1988**, *17*, 575–586.

(38) Bolyos, E.; Lawrence, D.; Nordin, A.*Proceedings from the Third International Disposal Conference*, Kariskoga, Sweden, Nov 10−11, 2003.

(39) Knudsen, J. N.; Jensen, P. A.; Lin, W.; Dam-Johansen, K. *Energy Fuels* **2005**, *19*, 606–617.

(40) Jenkins, B. M.; Bakker, R. R.; Wei, J. B. *Biomass Bioenergy* **1996**, *10*, 177–200.

(41) Srinivasachar, S.; Helble, J. J.; O., D.; Domazetis, G. *Prog. Energy Combust. Sci.* **1990**, *16*, 303–309.

(42) Dayton, D. C.; Jenkins, B. M.; Turn, S. Q.; Bakker, R. R.; Williams, R. B.; Belle-Qudry, D.; Hill, L. M. *Energy Fuels* **1999**, *13*, 860–870.

(43) Telfer, M. A.; Zhang, D. K. *Energy Fuels* **1998**, *12*, 1135–1141.

(44) Sander, B. *Biomass Bioenergy* **1997**, *12*, 177–183.

(45) Jenkins, B. M.; Baxter, L. L.; T. R., M., Jr.; Miles, T. R. *Fuel Process. Technol.* **1998**, *54*, 17–46.

(46) Davidsson, K. O.; Korsgren, J. G.; Pettersson, J. B. C.; Jäglid, U. *Fuel* **2002**, *81*, 137–142.

(47) *Handbook of Chemistry and Physics*, 90th ed.; Lide, D. R., Ed.; Chemical Rubber Company: Boca Raton, FL, 2009−2010; Chapter 4, pp 81−84, ISBN: 978-1-4200-9084-0.

(48) Davidsson, K. O.; Pettersson, J. B. C.; Nilsson, R. *Fuel* **2002**, *81*, 259–262.

(49) Christensen, K. A.; Stenholm, M.; Livbjerg, H. *J. Aerosol Sci.* **1998**, *29*, 421–444.

(50) Jensen, A.; Dam-Johansen, K. *Energy Fuels* **1998**, *12*, 929–938.